User Correlation Using Rotating Planar Antenna Arrays for Line-of-Sight Massive Multiple Input Multiple Output

G. C. Eze[1*], M. A. Ahaneku [2] and V. C. Chijindu [3]

[1]Department of Electronic and Electrical Engineering, Federal Polytechnic, Oko, Anambra State, Nigeria
[2,3]Department of Electronic and Computer Engineering, University of Nigeria, Nsukka, Enugu State, Nigeria.

ABSTRACT: This work investigates an array antenna rotation (AAR) technique in order to minimize inter-user correlation for massive multiple-input-multiple-output (MIMO) in pure line-of-sight (LoS) environment. Traditional planar arrays have better signal separation performance than linear arrays and can create three dimensional beams. However, when the angular separation of some signals between the users from/to the base station (BS) are small, the interference suppression (i.e., signal separation) performance degenerates since the projection points onto horizontal and vertical axes of several antenna elements overlap and spatial resolution along each axis is degraded. The aim is to improve inter-user correlation performance via mechanical rotation angle optimization. We propose a recursive bisection algorithm for rotation angle optimization by finding the optimal antenna rotation angle. Simulation results show in particular that the rotation of antenna body at the BS has inter-user correlation impact on large number of antennas in both horizontal and vertical resolutions. The 5th percentile inter-user correlation values of 8×16, 16×32, 32×64, 64×128 and 128×136 AAR configurations are 0.96, 0.86, 0.53, 0.03, and 0.00, respectively. This means that inter-user correlation increases with decrease in number of antennas and can be achieved in practice. Finally, the spatial decorrelation of AAR is superior compared to parallelogram planar array (PPA) and uniform planar array (UPA) because of mechanical rotation of antenna body.

KEYWORDS: *Array antenna rotation, inter-user correlation, Line-of-Sight, massive MIMO, collinear channel.*

[Received May 16, 2025; Revised June 9, 2025; Accepted July 7, 2025] Print ISSN: 0189-9546 | Online ISSN: 2437-2110

I. INTRODUCTION

MIMO has been identified as the primary enabling technology for mobile wireless communications, both now and in the future (Henrik et al, 2024). Massive MIMO may operate in both dense scattering environments (i.i.d. Rayleigh fading channels) and non-scattering conditions, such as pure line-of-sight (LoS) propagation (Pratschner et al, 2019). The substantial impact on a massive MIMO network's performance is primarily determined by the correlation or collinearity of user channels. In dense scattering scenarios, channels are asymptotically orthogonal characterized because of the law of large numbers while in LoS, the transmitting beams are focused directly on the users (Björnson et al, 2017). The LoS propagation channel and antenna arrays create spatial channel correlation or inter-user correlation. Inter-user correlation exists in practical massive MIMO for two reasons in order to boost network's capacity. First, the practical propagation scenarios may not produce requisite scatters. Second, there may be no enough space for the separation of antenna elements at the base station (BS) and the limited physical sizes of the mobile users. The challenges of separating closely located users with distance are reviewed with some related works.

The utilization of distance between the users was applied by both Shikhantsov et al. (2021) and Pratschner et al. (2020) in order to exploit the spatial collinearity in massive MIMO channels. Shikhantsov et al. (2021) presented that the measured channels were reducing with the inter-user distance. While Pratschner et al. (2020) demonstrated that users at long distances, a scattering environment creates spatially correlated or collinear channels; in this scenario, massive MIMO with LoS is better than massive MIMO without LoS. This is due to the fact that in both urban macro- and micro-cells (UMa, UMi), the chance of LoS decreases as the link distance increases. Additionally, it has been demonstrated that LoS communication is more dependable at millimeter-wave MIMO due to increased transmission loss, diffraction, and penetration losses. On the other hand, any realistic channel model may overestimate user correlation if the LoS channel model is applied without user correlation for performance analysis. Pratschner et al. (2019) presented that user correlation of pure LoS is implicitly obtained through geometry. Since multi-user MIMO networks are considered to be massive MIMO, user channels correlation is vital for the communications network's performance. The user correlation depends majorly on the angular spread and the antenna array geometry (aperture, antenna inter-element spacing).

Farsaei et al. (2020) investigated the problem of spatial separation in MIMO networks depicting those two users experiencing collinear channels can be separated in LoS

*Corresponding author: *eze.gerald@federalpolyoko.edu.ng*

doi: http://dx.doi.org/10.63746/njtd.v22i3.3530

channel environments. Also, the same researchers acquired an improved uniform linear array (ULA) using probability analysis for LoS massive MIMO with the two users possessing a correlation threshold value of 0.64. The two users are considered to be in x-y plane and assumed to be separated by distance and azimuth angle from the first element of the antenna array. Numerical results show that the improved ULA outperformed half-wavelength (½λ) ULA by 9.90 bits/channel of spectral efficiency (SE) without dropping a user and 1.43 bits/channel of SE with dropping one user, both employing zero forcing (ZF) precoder. However, due to the substantial spatial changes generated by the environment, the advantage of sparse arrays over the conventional ULA with ½λ inter-element spacing has proved insignificant in a rich scattering environment. Yang and Marzetta (2017) demonstrated that in a non-favorable propagation environment, there is a substantial likelihood that some users' channels in LoS massive MIMO are strongly collinear. According to Gao et al. (2011), the SE of both linear and nonlinear precoding schemes decreases as a result of the high collinearity.

As shown in Farsaei et al. (2019), the SE degrades significantly to the high collinearity in LoS scenario with max-min power control. Furthermore, the same authors illustrated how the signal to noise ratio (SNR) with max-min power management will drastically decrease when there is only one pair of strongly collinear users. Same researchers used dropping algorithms to study extremely collinear scenarios in LoS environments with max-min power control. The results of the studies showed that when the number of high-correlation users drops slightly, massive MIMO with max-min power management performs similarly under i.i.d Rayleigh and LoS channels.

In addition, spatially consistent channel models are required to investigate the effects of co-located users' spatial collinearity. For instance, when two users are physically nearby to one another, they experience a collinear channel, which is known as a spatial consistency channel. By altering the angular spread of multipath components (MPCs), Pratschner et al. (2019) managed the collinearity between MIMO channels without using a spatially consistent channel model. An exponential correlation model provides a user's channel collinearity matrix, whereas Chien et al. (2018) depicted that users are assumed to be non-collinear. Similarly, a matrix-based correlation model is used by Honda (2021) to determine a collinear MIMO channel. The Gaussian local scattering model by Björnson et al. (2017), provides the inter-user channel collinearity matrix (Özdogan et al, 2018) while geometry yields the pure LoS component. Pratschner et al. (2020) demonstrated that the location of scattering objects visible to the user (i.e., receiver) determines the value of spatial decorrelation and the collinearity behavior with distance.

These aforementioned reviewed studies resolved the issue of channel correlation for massive MIMO with various antenna configurations, including horizontal, vertical, and planar arrays in LoS scenarios, sensitive to inter-user distances without the assuming the angle spread between the users. The phase rotation of the signals received by each antenna element can be processed independently by these antenna arrays with minimal complexity. However, due to inter-user correlation, the linear (horizontal or vertical) array performs worse in signal separation than the planar array (Akao et al, 2019; Maruta et al, 2017). The parallelogram planar array (PPA), which was proposed by Maruta et al. (2017) and Arai et al. (2017), was utilized to successfully lower the inter-user correlation for massive MIMO in LoS scenario. The suggested PPA by Arai et al. (2017) has the ability to regulate mutual coupling, excessive antenna scale, and grating-lobe placements. According to numerical results, the suggested PPA may lower the inter-user correlation at CDF=50% value by 80% when compared to a uniform cylindrical array (UCA) and 75% when compared to a uniform planar array (UPA). It also provides better signal-to-interference ratio (SIR) performance.

Comparative analyses between UCA and UPA for multi-user MIMO, beamforming and 3GPP 3-Dimensional channel model were studied by Shafie et al. (2024) and Riviello et al. (2024). Riviello et al. (2023) and Riviello et al. (2019) illustrated the potential benefits of UCA over UPA in realistic 3-Dimensional environments. Simulative results in terms of per-user rate, sum-rate, SE, and outage for outdoor non-LoS, outdoor LoS, and indoor users were presented. Lin et al. (2021) and Lin et al. (2020) proposed a hybrid UCA for massive Internet of Things (IoT) networks, and also used channel plus direction of arrival (DOA) estimation techniques for the proposed hybrid UCA.

In order to enhance DOA estimation method, Hanada and Maruta (2020) used mechanical rotation of UPA to enhance estimation accuracy. Mechanical rotation of UPA with small number of antenna elements (i.e., 2×4 and 4×4) was carried out by Hanada and Maruta (2020), and Akao et al. (2019) to minimize channel spatial collinearity between users without put into consideration the characteristics and behaviour of large number of antenna elements at the BS. Meanwhile, PPA limitation is determined, if the antenna architecture is optimally chosen based on user distribution in inclined plane due to PPA antenna arrangement is fixed, then additional decorrelation becomes essential. As a result, the planar array using mechanical antenna body rotation is the main focus here. Investigating the inter-user decorrelation effect of array antenna rotation (AAR) for massive MIMO in a LoS scenario is the aim of this work.

The major contributions of this work are:

- To analyse the impact of user correlation of rotating antenna body in pure LoS massive MIMO depending on inter-user angular separation.
- To use recursive bisection method for angle rotation optimization.

The rest of this work is structured as follows: Section II illustrates the system model of antenna array structure; Section III describes the material and method including channel correlation and its metrics, plus proposed recursive bisection method for angle rotation optimization using MATLAB simulation. In Section IV, the results and discussions are presented. Finally, Section V provides the conclusions extracted from this work.

II. SYSTEM MODEL

In LoS massive MIMO network, antennas are the main components of wireless channel. An antenna consists of single

or multiple radiating elements which are connected to the same radio frequency (RF) signal. The phase and amplitude of the signal received by individual antenna element are not dependently controlled (Björnson et al, 2017). Moreover, a typical configuration of antenna elements is classified into linear, cylindrical (or circular) and planar (or rectangular) array. Antenna arrays are designed in shapes and different sizes depending on the area coverage and carrier frequency.

A. Antenna Array Structure

An antenna array is composed of multiple antennas with individual RF chains, which are uniformly arranged. The frequently used arrays in LoS massive MIMO networks are either (vertical/horizontal) linear or (parallelogram/sparse tiled) planar arrays (Björnson et al, 2017). To compute channel correlation |ρ| for different antenna array structures such as UPA, PPA, and AAR, the modelling for different antenna elements ($M_H \times M_V$) of UPA, PPA, and AAR at the BS must be determined. This can be obtained by using needed mathematical expression for the modelling procedure.

1) Uniform planar array

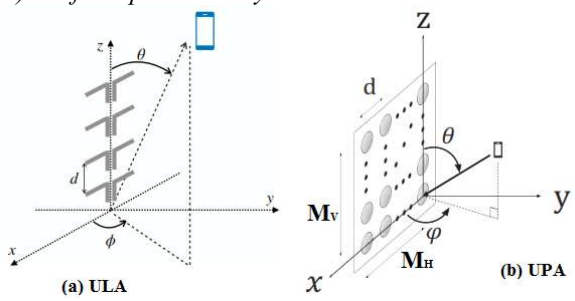

Figure 1: ULA and UPA structure (Hanada and Maruta, 2020)

ULA and UPA geometries with antenna elements along z-axis and x-axis, and inter-element distance (d) between the elements at BS are illustrated in figure 1. BS can have a large number of antenna elements. With J antenna elements (M_H) in each column and I antenna elements (M_V) in each row (Xu et al, 2017), we assume that I × J UPA is in the x-z plane (see Fig. 2). As determined by Akao et al. (2019), (1) can be used to indicate the UPA array factor $a_{ij}(\theta,\varphi)$ that the (i,j)th antenna element ($1 < i \leq I$, $1 \leq j \leq J$) transmits (or receives) to (or from) the user's signal.

$$a_{ij}(\theta,\varphi) = \exp\left[\frac{2\pi}{\lambda} d(j-1)\cos\varphi\sin\theta + (i-1)\cos\theta\right] \quad (1)$$

Where λ is the wavelength and d is the inter-element spacing. In planar array configuration, 3-Dimensional beam is performed, while in ULA configuration, 2-Dimensional beam is performed. As a result, the planar array arrangement performs better at signal separation than the ULA overall. But if the arrival angles are small, the signal separation performance of the ULA is good than the planar array configuration. For example, it is difficult to eliminate signals in the elevation domain if θ is small. It degrades the horizontal resolution of the spatial channel in the UPA in comparison to a horizontal array (1× I J) (Akao et al, 2019). However, two users' signals will interfere with one another significantly if they are received from similar θ and φ.

2) Parallelogram planar array

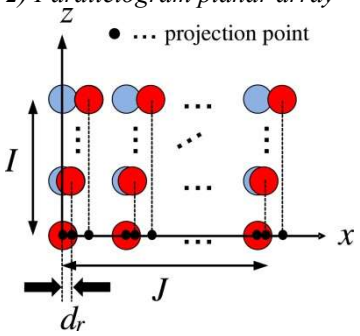

Figure 2: UPA (blue) and PPA (red) structure (Akao et al, 2019)

PPA antenna arrangement involves giving each row of antenna elements a column-wise offset (Maruta et al, 2017). Each row in figure 2's representation of the PPA structure is routinely offset from its neighbours. Therefore, virtual inter-element spacing (VIS), which is aligned in the same interval without overlap, is the term used to describe the projection locations of all antenna components on the horizontal axis. Each antenna element is on the same column, in contrast to the conventional UPA, which is responsible for the decrease in the channel spatial correlation. The enhancement in the spatial channel's horizontal resolution and the elimination of unwanted grating robes make this possible. The PPA array factor a_{ij} (θ,φ) that the (i,j) th antenna element ($1 \leq i \leq I$, $1 \leq j \leq J$) transmits (or receives) to (or from) user's signal may be expressed in (2) as obtained by Akao et al. (2019).

$$a_{ij}(\theta,\varphi) = exp\left[\frac{2\pi}{\lambda} d[(j-1) + (i-1)d_r]cos\varphi sin\theta + (i-1)cos\theta\right] \quad (2)$$

Where d_r is the column-wise offset to provide the PPA structure. Maruta et al. (2017) shown that PPA can decrease the inter-user correlation without any rise in processing load.

3) Array antenna rotation

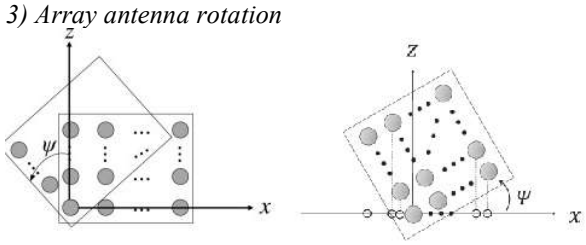

Figure 3: AAR structure (Akao et al, 2019; Hanada and Maruta, 2020)

AAR is a concept developed from the inspiration of designing PPA structure. Figure 3 shows the schematic structure of AAR, a simplified method that mechanically rotates the antenna body. The reference antenna element is rotated around the UPA or PPA structure (i, j = 1, 1). Every rotation creates an offsetting for every row and column. The (i,j)th antenna element ($1 \leq i \leq I$, $1 \leq j \leq J$) broadcasts (or receives) to (or from) the user's signal, and the AAR array factor a_ij (θ,φ,ψ) can be stated in (3) as found by Akao et al. (2019) .

$$a_{ij}(\theta,\varphi,\psi) = \exp\left[\frac{2\pi j}{\lambda} d[(i-1)\cos\varphi - (j-1)\sin\psi]\cos\theta + [(i-1)\sin\psi + (j-1)\cos\psi]\cos\varphi\sin\theta\right] \quad (3)$$

Where ψ represents rotation angle of the antenna body. Thus, AAR technique can produce similar effect as the PPA, where each column and row is regularly offset from its neighbours. Furthermore, ψ has effect in controlling inter-user correlation. AAR technique is now widely used and applied in aeronautical systems across the world (Greving et al, 2012). Implementation and fabrication of mechanical controlled antenna body is considered to be possible these days. Since spatial channel correlation is a vital property of LoS massive MIMO, we will now derive a channel correlation model that will be used in the numerical analysis.

B. Channel Correlation

Channel correlation is clearly a measurement of how rich the scattering of massive MIMO channel may be. Channel correlation may be divided into two groups namely intra-user correlation and inter-user correlation. Intra-user correlation occurs between the users of similar channels. Thus, intra-user correlation can be used in the detection of the user locations. Inter-user correlation occurs between the users of different channels and its performance deteriorates. Inter-user correlation is a type of statistical channel analysis.

III. MATERIALS AND METHOD

We consider two users (or receivers) and a BS (or transmitter) equipped with different antenna elements ($M_H \times M_V$) of AAR, PPA, and UPA on the x-z plane in the LoS scenario. The elevation (or zenith) and azimuth angles of the two users are assumed to be (θ_1, φ_1) and(θ_2, φ_2), respectively. Both the elevation and azimuth domains are used to perform the beamforming function. We considered a maximum ratio (MR) transmission precoding in the case of two user channels. The spatial correlation between the user channels: desired user (a_{ij}^{D}) and interfering or undesired user (a_{ij}^{U}) is given by Pratschner et al. (2019) and Björnson et al. (2017):

$$\rho = \frac{\left|a_{ij}^{D}(\theta_1,\varphi_1)^{H} a_{ij}^{U}(\theta_2,\varphi_2)\right|^2}{\left\|a_{ij}^{D}(\theta_1,\varphi_1)\right\|^2 \left\|a_{ij}^{U}(\theta_2,\varphi_2)\right\|^2} \quad (4a)$$

Where ρ is the metric for user correlation and the inner product of normalized a_{ij}^{D} and a_{ij}^{U} for a given coherence interval. Our focus is to investigate the user correlation of the array responses.

$$|\rho| = \frac{1}{M}|a(\theta_1,\varphi_1)^{H} a(\theta_2,\varphi_2)| \quad (4b)$$

Where M denotes the number of antennas and M equals ($M_H \times M_V$). Therefore, we introduce the ρ(ψ) as

$$\rho(\psi) = \frac{\left|a_{ij}^{D}(\theta_1,\varphi_1,\psi)^{H} a_{ij}^{U}(\theta_2,\varphi_2,\psi)\right|^2}{\left\|a_{ij}^{D}(\theta_1,\varphi_1,\psi)\right\|^2 \left\|a_{ij}^{U}(\theta_2,\varphi_2,\psi)\right\|^2} \quad (4c)$$

Where the steering matrices are $a_{ij}^{D}(\theta_1,\varphi_1,\psi)$ and $a_{ij}^{U}(\theta_2,\varphi_2,\psi)$ for desired user and interfering user. The following steps were used effectively for the computation of user correlation ρ for different antenna array structures throughout the course of this work.

- Step 1: User correlation ρ for AAR with different antenna elements ($M_H \times M_V$) at the BS is computed using AAR array factor (3) and equation (4c).
- Step 2: User correlation ρ for PPA with different antenna elements ($M_H \times M_V$) at the BS is computed using PPA array factor (2) and equation (4a).
- Step 3: User correlation ρ for UPA with different antenna elements ($M_H \times M_V$) at the BS is computed using UPA array factor (1) and equation (4a).

A. User correlation Optimization Problem

This section aims at maximizing and minimizing the spatial channel correlation for the two users by utilizing θ, φ, and ψ. In the following, for maximizing user correlation, we convert (4c) into the equivalent problem form of

$$\text{maximum } \rho$$
$$\text{s.t } \rho\left\|a_{ij}^{D}(\theta_1,\varphi_1,\psi)\right\|^2\left\|a_{ij}^{U}(\theta_2,\varphi_2,\psi)\right\|^2 - \left|a_{ij}^{D}(\theta_1,\varphi_1,\psi)^{H} a_{ij}^{U}(\theta_2,\varphi_2,\psi)\right|^2 \leq 1. \quad (5a)$$

For minimizing user correlation, we convert (4c) into the equivalent problem form of

$$\text{minimize } \rho$$
$$\text{s.t } \left|a_{ij}^{D}(\theta_1,\varphi_1,\psi)^{H} a_{ij}^{U}(\theta_2,\varphi_2,\psi)\right|^2 - \rho\left\|a_{ij}^{D}(\theta_1,\varphi_1,\psi)\right\|^2\left\|a_{ij}^{U}(\theta_2,\varphi_2,\psi)\right\|^2 \geq 0. \quad (5b)$$

This user correlation metric is bounded as $0 \leq \rho(\psi) \leq 1$, where a value of 0 identifies channel inner product as uncorrelated or orthogonal (i.e., the inter-user interference disappears) and a value of 1 identifies channel inner product as correlated or collinear. The inner product of desired and undesired users does not tend to zero in merit of favorable propagation because the channel norms increase with M; that is, the channel directions become non-collinear, but not the array responses.

1) Antenna-element spacing and array size

The user collinearity of equation (4b) characterises as function of angular separation between the two users and antenna array geometry (Björnson et al, 2017).We facilitate identification and present the quantities found by Farsaei et al. (2020) and Björnson et al. (2017).

$$\Omega = \sin(\theta_1) - \sin(\theta_2) \quad (6a)$$
$$\Psi = \cos(\theta_1)\sin(\varphi_1) - \cos(\theta_2)\sin(\varphi_2) \quad (6b)$$

Where the elevation and azimuth angles are confined within the interval [-π/2, π/2], it follows that Ω, Ψ ∈ [-2, 2]. The distributions of these quantities are non-uniform and dependent on the distribution of the users.

$$S(\Omega) = \left|\frac{\sin(\pi M_V d_V \Omega)}{M_V \sin(\pi d_V \Omega)}\right| \quad (7a)$$
$$T(\Psi) = \left|\frac{\sin(\pi M_H d_H \Psi)}{M_H \sin(\pi d_H \Psi)}\right| \quad (7b)$$

Where M_V and M_H are number of vertical and horizontal antennas, d_V and d_H represent vertical and horizontal inter-element spacing (in multiples of the wavelength). The normalized array height and width are defined by $M_V d_V$ and $M_H d_H$ respectively. The impact values of Ω, Ψ, S(Ω) and T(Ψ) are of practical importance. The angular separation of the users in the elevation domain is dependent on S(Ω) while all azimuth and elevation angles are dependent on T(Ψ).The characteristics of T(Ψ) is identical unlike S(Ω) that is not identical. Therefore, the user correlation can be denoted as the product of two functions S(Ω) and T(Ψ). User correlation is found by:

$$|\rho| = S(\Omega) \times T(\Psi) \quad (8)$$

In contrast, the UPA and vertical ULA exhibit higher |ρ| because of smaller vertical angular spread between users i.e. it is difficult to separate users in the elevation domain than in the azimuth domain. In fig. 4, |ρ| is expressed as a function of Ψ for a UPA of M = (8×16) antennas with the equal inter-element spacing between respective M_H and M_V antennas ($d_H = d_V$).

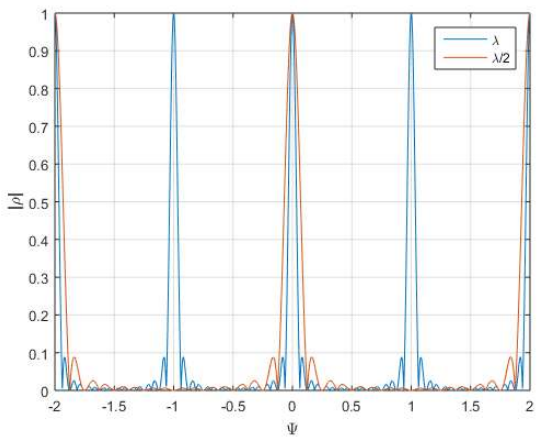

Figure 4: The channel correlation|ρ| function against Ψ for a UPA with M_H = 8, M_V = 16, and different inter-element spacing (using $d_H = d_V$).

The blue and red lines are associated with $d_H = \lambda$ and $d_H = \lambda/2$, respectively. The function $|\rho|$ has the main-lobes around the origin with a width of $\frac{2}{M_H d_H}$ (0.25, 0.5) and periodic with period $\frac{1}{d_H}$ (1, 2) while all other lobes have much smaller maximum values. This shows the UPA is not able to separate desired and undesired users whenever the signals of desired and undesired users arrive from similar θ and φ, they will interfere with each other strongly. On the other hand, the angular resolution of the UPA is improved and the grating lobes appear by increasing d_H from $\lambda/2$ to λ.

B. Correlation Matrix Distance (CMD)

Correlation matrix distance (CMD) is the channel matrix collinearity and a type of statistical channel analysis. Thus, we define the CMD (Pratschner et al., 2020) between the two correlation matrices $a_{ij}^{D}(\theta_1, \varphi_1, \psi)$and $a_{ij}^{U}(\theta_2, \varphi_2, \psi)$ as

$$\mathrm{CMD}(a_{ij}^{D}, a_{ij}^{U}) = \frac{\mathrm{trace}\left(a_{ij}^{D}(\theta_1,\varphi_1,\psi)^{H} a_{ij}^{U}(\theta_2,\varphi_2,\psi)\right)}{\left\|a_{ij}^{D}(\theta_1,\varphi_1,\psi)\right\|\left\|a_{ij}^{U}(\theta_2,\varphi_2,\psi)\right\|} \quad (9)$$

The range of the CMD metric is $0 \leq \mathrm{CMD} \leq 1$.If the matrices of a_{ij}^{D} and a_{ij}^{U} are correlated in the sense that $a_{ij}^{D} = c a_{ij}^{U}$ with $c \geq 0$, then the equality of the form CMD = 1. Massive MIMO channel experiments using large scale antenna arrays show that a non-stationary channel is not stationary throughout the array aperture (Pratschner et al., 2020; Pratschner et al., 2018). A common metric for stationarity is the CMD, which is equal to one for every conceivable position. Furthermore, a measured channel has measurement noise and is not perfectly stationary; the CMD is less than one (Pratschner et al., 2020*).*

C. Chordal Distance (CD)

User correlation matrices generally contain a mix of a few strong and many weak eigendirections. In some cases, the correlation matrix might possess a full rank, which has eigenspace that capture most of the energy. In order to define a metric for measuring orthogonality between two eigenspaces (Björnson et al, 2017), we consider the chordal distance (CD). The CD between two matrices $a_{ij}^{D}(\theta_1, \varphi_1, \psi)$ and $a_{ij}^{U}(\theta_2, \varphi_2, \psi)$ is introduced as obtained by Björnson et al (2017). $\mathrm{CD}(a_{ij}^{D}, a_{ij}^{U}) = \left\|a_{ij}^{D}(\theta_1, \varphi_1, \psi)a_{ij}^{D}(\theta_1, \varphi_1, \psi)^{H} - a_{ij}^{U}(\theta_2, \varphi_2, \psi)a_{ij}^{U}(\theta_1, \varphi_1, \psi)^{H}\right\|_F^2$ (10)

D. Signal Interference Ratio (SIR) and Achievable Spectral Efficiency (SE)

In order to illustrate the impact of user correlation on a LoS massive MIMO network, we present results for the achievable SE with the rotation angle in this section. Let us consider signal interference ratio (SIR) of user u, defined via the SINR with noise ($\sigma^2 = 0$).The expression for the effective SIR as given by Pratschner et al., (2020) and Pratschner et al., (2019) is expressed in (11a).

$$\mathrm{SIR}_u = \frac{p_u \left|\mathbb{E}\{a_u^H w_u\}\right|^2}{\sum_{k\neq u}^{U} p_k \left|\mathbb{E}\{a_u^H w_k\}\right|^2} \quad (11a)$$

Where p_k is the transmit power. Further, we apply equal transmit power to all users (i.e., $p_u = p_k$). In this work, we consider MR precoding, with a precoding vector of kth user calculated as

$$w_k = \frac{a_k}{\|a_k\|} \quad (11b)$$

Inserting a normalized MR precoder $w_u = \frac{a_u}{\|a_u\|}$ and w_k, therefore $\mathrm{SIR}_u = \left[\frac{\left|a_u^H a_k\right|^2}{\|a_u\|^2\|a_k\|^2}\right]^{-1}$ .Using the user correlation metric in (4) by inspection.

$$\mathrm{SIR}_u = [\rho(\psi)]^{-1} \quad (11c)$$

The achievable sum SE in bits/s/Hz is

$$\mathrm{SE} = \sum_{u=1}^{U} \log_2(1 + \mathrm{SIR}_u) \quad (11d)$$

The mean achievable sum SE for the case of two users with MR precoding is shown in Fig. 11. Inter-user correlation increases the sum SE since it reduces interference and ρ^2 is the inter-user interference power. Users that have similar inter-user correlation matrices interfere more with each other thereby creating larger variations in SE.

E. Rotation angle optimization based on proposed recursive bisection procedure

1) Problem formulation

This section analyzes the minimized maximum$\rho(\psi)$, which fluctuates based on the combination of θ, φ, and ψ. In order to reduce the user correlation, we must determine the ideal rotation angle,ψ_{OPT}. Furthermore, we propose a user correlation based rotation angle optimization method using recursive bisection procedure. Equation (4a) can be used to determine the user correlation between the desired and interfering users when the desired signal from the desired user and the interference signal from the undesirable user are present. $a_{ij}^{D}(\theta_1, \varphi_1, \psi)$ and $a_{ij}^{U}(\theta_2, \varphi_2, \psi)$ are functions of ψ, according to equation (4c). Improving the signal separation performance, $\rho(\psi)$ between users with the highest $\rho(\psi)$ value should be minimized. In order to reduce the highest mutual inner product between users, we take into consideration a min–max fairness technique. It can be expressed as solving the min-max fairness problem as follows:

$$\min_{\psi} \max_{\rho} \rho(\psi)$$
$$\text{s.t. } 0 \leq \rho(\psi) \leq 1 \quad (12)$$

By solving a series of linear feasibility issues, Algorithm 1 achieves the global optimality of the min–max problem to a

tolerance $\Delta = 10^{-4}$. The search space for the ψ value is cut in half with each iteration since the algorithm's outer while-loop conducts a recursive bisection search for the ideal ψ value. While shifting ψ by Δ ψ, these procedures are repeated, and ψ_{OPT} is sought. As a result, the convergence happens quite quickly. Figures 5 and 6 illustrate an expanded flowchart of recursive bisection method based on rotation angle optimization.

Algorithm 1: Recursive bisection method based on Rotation angle optimization.

RESULT: Solve the optimization problem in (12).

Step 0:

INPUT: $\psi = [\psi_1, \psi_2, \ldots, \psi_n]$ and Tolerance value Δ

SET: $\psi_{LOWER} = \min(\psi)$

SET: $\psi_{UPPER} = \max(\psi)$

//Initialize the Channel Correlation Matrices

$\rho_{LOWER} = AAR(\theta_{12}, \varphi_{12}, \psi_{LOWER})$

$\rho_{UPPER} = AAR(\theta_{12}, \varphi_{12}, \psi_{UPPER})$

SET: n = 1 //Initialize the Counter

SET: $\psi_{MIDPOINT\_OLD} = 0$

Step 1:

If $|\psi_{LOWER} - \psi_{UPPER}| > \Delta$ go to step 2, otherwise go to step 0 or stop

Step 2:

Compute /*Recursive Bisection over potential ρ values */

$\psi_{MIDPOINT} = (\psi_{LOWER} + \psi_{UPPER})/2$

$\rho_{MIDPOINT} = AAR(\theta_{12}, \varphi_{12}, \psi_{MIDPOINT})$

$\psi_{MIDPOINT\_LOWER} = (\psi_{LOWER} + \psi_{MIDPOINT})/2$

$\rho_{MIDPOINT\_LOWER} = AAR(\theta_{12}, \varphi_{12}, \psi_{MIDPOINT\_LOWER})$

$\psi_{MIDPOINT\_UPPER} = (\psi_{UPPER} + \psi_{MIDPOINT})/2$

$\rho_{MIDPOINT\_UPPER} = AAR(\theta_{12}, \varphi_{12}, \psi_{MIDPOINT\_UPPER})$

Step 3:

If $\rho_{MIDPOINT_{LOWER}} \leq \rho_{MIDPOINT}$

OR

$\rho_{MIDPOINT} \leq \rho_{MIDPOINT\_UPPER}$

SET: $\psi_{LOWER} = \psi_{MIDPOINT\_LOWER}$

Else If $\rho_{MIDPOINT_{LOWER}} \geq \rho_{MIDPOINT}$

OR

$\rho_{MIDPOINT} \geq \rho_{MIDPOINT\_UPPER}$

SET: $\psi_{UPPER} = \psi_{MIDPOINT\_UPPER}$

Else If $\rho_{MIDPOINT} \leq \max(\rho_{MIDPOINT\_LOWER}, \rho_{MIDPOINT\_UPPER})$

SET: $\psi_{UPPER} = \psi_{MIDPOINT\_UPPER}$

SET: $\psi_{LOWER} = \psi_{MIDPOINT\_LOWER}$

End If

SET: $\psi_{MIDPOINT\_OLD} = \psi_{MIDPOINT}$

UPDATE: $\Delta_{ANGLE} = |\psi_{LOWER} - \psi_{UPPER}|$

SET: n = n + 1

Step 4:

If $\Delta_{ANGLE} > \Delta$ *go to step 2, otherwise OUTPUT:* $\psi_{OPT} = \psi_{MIDPOINT}$

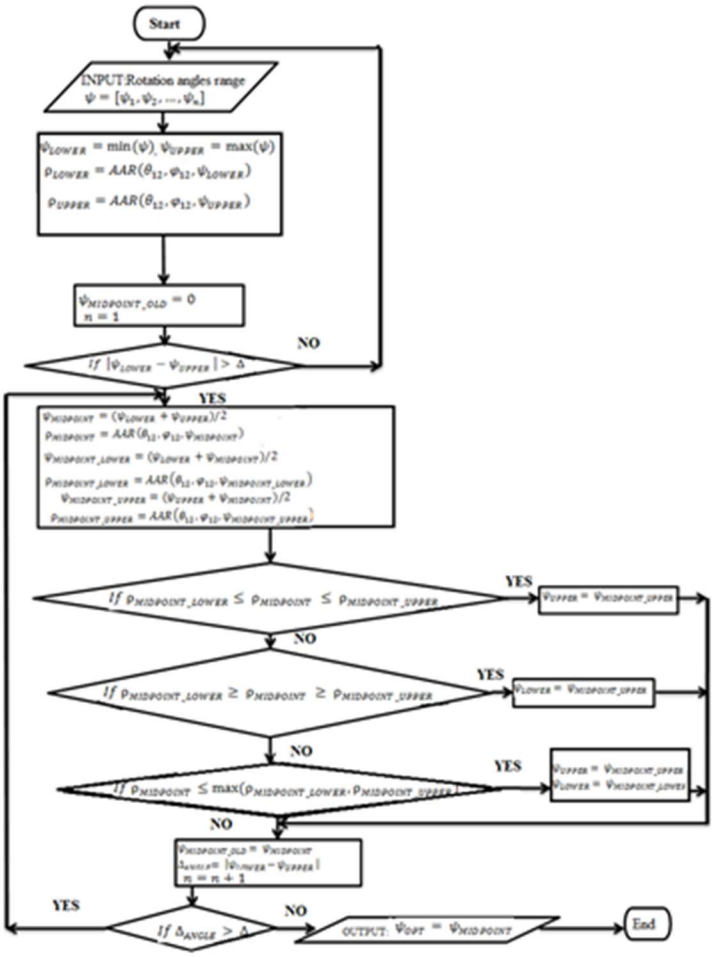

Figure 5: Flowchart of Algorithm 1

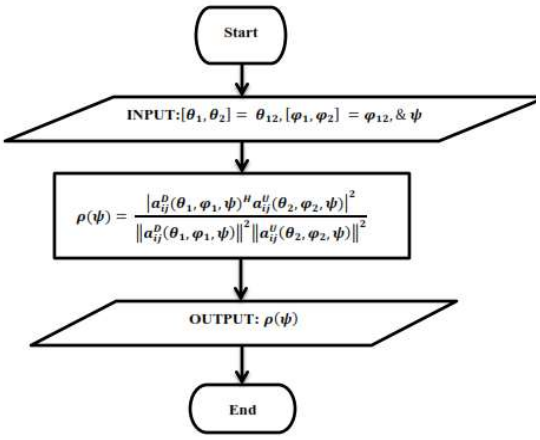

Figure 6: Flowchart of Algorithm 2

Algorithm 2: *AAR method*

RESULT: Find ρ

//Initialize the Elevation, Azimuth and Rotation Angles

Step 0:

INPUT: $\theta_{12} \Rightarrow [\theta_1, \theta_2], \varphi_{12} \Rightarrow [\varphi_1, \varphi_2] \& \psi$

Step 1:

CALCULATE: Solve ρ in (4) OR use optimization Problem either in (5a) or (5b)

$$\rho(\psi) = \frac{\left|a_{ij}^{D}(\theta_1, \varphi_1, \psi)^{H} a_{ij}^{U}(\theta_2, \varphi_2, \psi)\right|^2}{\left\|a_{ij}^{D}(\theta_1, \varphi_1, \psi)\right\|^2 \left\|a_{ij}^{U}(\theta_2, \varphi_2, \psi)\right\|^2}$$

Step 3:
OUTPUT: $\rho(\psi)$

F. Simulation

In this section, we consider a three-dimensional pure LoS model (Björnson et al., 2017) and the case that the locations of the two users are specified by the elevation and azimuth angles, (θ_1, θ_2) = [45°(π/4), 22.5°(π/8)] and (φ_1, φ_2) = [45°(π/4), 22.5°(π/8)] respectively. Simulations/numerical analyses are carried out using MATLAB 2023b software for the $\rho(\psi)$ in (4) and set the number of antenna elements $(M_H \times M_V)$ = 8 × 16, 16 × 32, 32 × 64, 64 × 128, 128 × 136 for antenna array structures. Rotating angle (ψ) is altered from -180° to 180°, shifting ψ by 1°granularity. MR signal processing scheme is considered for the desired user and interfering user due to its low complexity. Patch antenna is assumed in this simulation in order to remove the influence of polarized waves. Table 1 lists the numerical analysis parameters.

Table 1: Simulation parameters

Parameter	Value
Number of Users	2
Signal processing scheme	MR
Array structure	UPA, PPA, AAR
Antenna elements $(\boldsymbol{M_H \times M_V})$	8×16,16×32,32×64, 64×128,128×136
Inter-element spacing (d)	λ/2
Column-wise offset $(\boldsymbol{d_r})$	λ/5 or 2 λ
For PPA structure	
Elevation Angles $(\boldsymbol{\theta_1, \theta_2})$	22.5° (π/8), 45° (π/4)
Azimuth Angles $(\boldsymbol{\varphi_1, \varphi_2})$	22.5° (π/8), 45° (π/4)
Rotation Angle $(\boldsymbol{\psi})$	-180° to 180°
Shift Angle $(\Delta\boldsymbol{\psi})$	1°

IV. RESULTS AND DISCUSSION

A. Impact of user correlation on AAR structure

User correlation is a statistical channel analysis metric used to measure inner product of two normalized users' channels. This metric is expressed in equations (3) and (4); we conducted numerical simulation of |ρ| by changing the rotating angle in the pure LoS massive MIMO network. As shown in figure 7, |ρ| is a function of ψ° with different elevation angles (θ_1= 22.5°, θ_2= 45°) and same azimuth angles (φ_1, φ_2) at 45° for different AAR configurations ($M_H \times M_V$). The fluctuation of |ρ| performance is symmetrical.

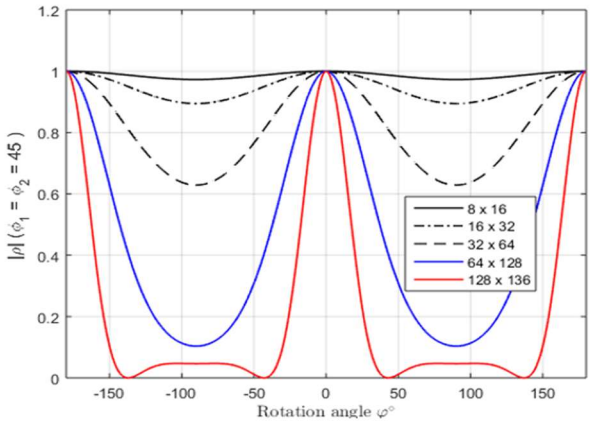

Figure 7: Channel correlation |ρ| for different AAR configurations ($M_H \times M_V$) vs. Rotation angle (ψ°) with equaled azimuth angles ($\varphi_1 = \varphi_2$ = 45°) and unequalled elevation angles ($\theta_1 \neq \theta_2$).

The function |ρ| of different antenna arrays is equal to 1 at ψ = 0° (with reflecting rotation angles at ψ = -180° and ψ = 180°) as presented in figure 7 and table 2. This shows that all the antenna elements projection points that are aligned on the horizontal axis do not overlap with the rotating of the antenna body because of vertical resolution. Hence, the spatial resolution is improved. We observe that the pure LoS massive MIMO channel is spatially consistent. In case of AAR configuration of 8 × 16, |ρ| is highly collinear (|ρ| ≈ 1) at all ψ which means that rotating of the antenna body does not have impact on |ρ| followed by spatial behavior of 16 × 32 and 32 × 64 AAR configurations that have the minimum values of |ρ| > 0.6. Meanwhile, in case of 64 × 128 and 128 × 136 AAR configurations, the rotating of the antenna body affects |ρ| because of their minimum values of |ρ| ≤ 0.1. By going from ψ = -40° to ψ = 0°, the |ρ| of 64 × 128 and 128 × 136 antenna arrays correlated exponentially and decorrelated exponentially from ψ = 0° to ψ = 40°.

Table 2: Elevation Domain

$(\boldsymbol{\theta_1, \theta_2})$	$\boldsymbol{\varphi_1 = \varphi_2}$	$\boldsymbol{\psi}$ $(\boldsymbol{\rho(0°) = 1})$
22.5°,45°	25.7°(π/7)	0°
22.5°,45°	30°(π/6)	0°
22.5°,45°	36°(π/5)	0°
22.5°,45°	45°(π/4)	0°
22.5°,45°	60°(π/3)	0°

This goes a long way to show that the rotating of antenna body at BS has huge spatial correlation impact on large number of antennas ($M = M_H \times M_V$). In figure 8, $|\rho|$ is depicted as function of ψ° with different azimuth angles (φ_1= 22.5°, φ_2= 45°) and same elevation angles (θ_1, θ_2) at 45° for different AAR configurations $(M_H \times M_V)$. By observation, the $|\rho|$ performance is improved by rotating the antenna body for different AAR configurations $(M_H \times M_V)$. Moreover, the function $|\rho|$ of different AAR configurations $(M_H \times M_V)$ is equal to 1 at ψ = -55° (with mirror rotation angle at ψ = 125°) due to overlapping of projection points of antenna elements on

the horizontal axis (Akao *et al*., 2019) and the spatial resolution is degraded.

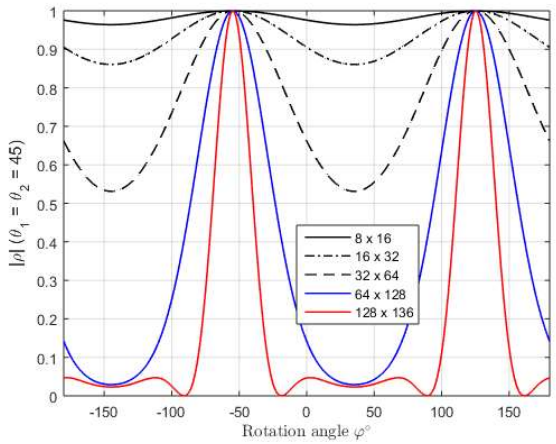

Figure 8: Channel correlation$|\rho|$ for different AAR configurations $(M_H \times M_V)$ vs. Rotation angle ($\psi°$) with unequaled azimuth angles ($\varphi_1 \neq \varphi_2$) and equaled elevation angles ($\theta_1 = \theta_2 = 45°$).

Hence, the desired user is coherently precoded or combined by the MR precoding or combining (just as the interfering user) because of smaller horizontal angular spread between users. Thus, the horizontal resolution works in pure LoS massive MIMO by shifting ψ to a particular value where $\rho(\psi°) = 1$ as presented in table 3, while in the vertical resolution, $\rho(0°) = 1$ at $\psi = 0°$ with no shifting (see table 2).

Table 3: Azimuth Domain

(φ_1, φ_2)	$\theta_1 = \theta_2$	ψ $(\rho(\psi) = 1)$
22.5°,45°	90°(π/2)	−45°
22.5°,45°	60°(π/3)	−50°
22.5°,45°	45°(π/4)	−55°
22.5°,45°	36°(π/5)	−60°
22.5°,45°	30°(π/6)	−63°
22.5°,45°	25.7°(π/7)	−67°
22.5°,45°	22.5(π/8)	−69°

From the table 3, as same elevation angles decrease, while rotating angle is increased by shifting ψ to the left where $\rho(\psi°) = 1$. On the other hand, the minimum values of $|\rho|$ of $8 \times 16, 16 \times 32$, and 32×64 antenna arrays > 0.5 and the minimum values of $|\rho|$ of 64×128 and 128×136 antenna arrays ≤ 0.05. We can see that the minimum values of $|\rho|$ in the elevation domain ($\theta_1 \neq \theta_2$) is slightly greater than the minimum values of $|\rho|$ in azimuth domain ($\varphi_1 \neq \varphi_2$) because of vertical angular spread between the two users, i.e. user separation is generally more effective in the azimuth domain than in the elevation domain. Although, the $|\rho|$ characteristics behavior of different antenna arrays in figures 7 and 8 are similar. This observation validates the methodology of AAR formulation in (3).

B. Impact of CMD on AAR structure

CMD is also a type of statistical channel analysis metric used to measure inner product of two users' channels. This metric is expressed in equation (9) and we simulated CMD by increasing the rotation angle in the LoS massive MIMO network as shown figure 9. The CMD is plotted against the rotation angle in Fig. 9 for the different AAR configurations.

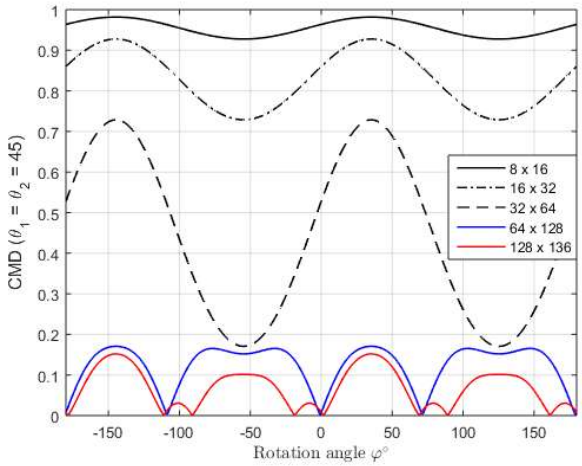

Figure 9: CMD for different AAR configurations $(M_H \times M_V)$ vs. Rotation angle ($\psi°$) with unequaled azimuth angles ($\varphi_1 \neq \varphi_2$) and equaled elevation angles ($\theta_1 = \theta_2 = 45°$).

Figure 9 shows CMD for different AAR configurations $(M_H \times M_V)$ as function of $\psi°$ for different azimuth angles (φ_1= 22.5°, φ_2= 45°) and same elevation angles (θ_1, θ_2) at 45°. CMD is considered flat and stationary for the LoS scenario because there are no scattering objects in between the BS and the user or around the user (Pratschner *et al*, 2020). For a stationary channel, the CMD is equal to one (CMD = 1) for all possible rotating angles. By observation, the average CMD values of 8×16, 16×32, 32×64, 64×128 and 128×136 antenna arrays are 0.96, 0.84, 0.44, 0.09 and 0.06, respectively. Please take note that low values of the CMD do not imply non-stationary channels. Since we compare the correlation of the desired user to the correlation of the interfering user as expressed in equation (9).The high values of the plotted CMD mean a high self-similarity of ρ (Pratschner *et al*, 2020). Thus, a CMD value of one indicate that the $\rho(\psi)$ is identical to LoS scenarios. Although low values of CMD do not indicate that the user channel performs non-stationary at ψ.

C. Impact of CD on AAR structure

This CD metric is expressed in equation (10). Simulation result in terms of CD over the rotating angle (ψ) is presented below. Figure 10 shows the chordal distance for rotating angle (ψ) between the correlation matrices of a desired user at azimuth angle 22.5° and that of interfering user at azimuth angle 45° with equaled elevation angles at 45° for different AAR configurations $(M_H \times M_V)$. The CD values of 8×16, 16×32, 32×64, 64×128 and 128×136 antenna arrays are 809.4, 4.96×10^4, 1.89×10^6, 1.15×10^8, and 5.77×10^8, respectively. We can observe that the CD increases with $M = M_H \times M_V$, because of the increased spatial resolution of the antenna

arrays, and with ψ since the $|\rho|$ matrices become increasingly different.

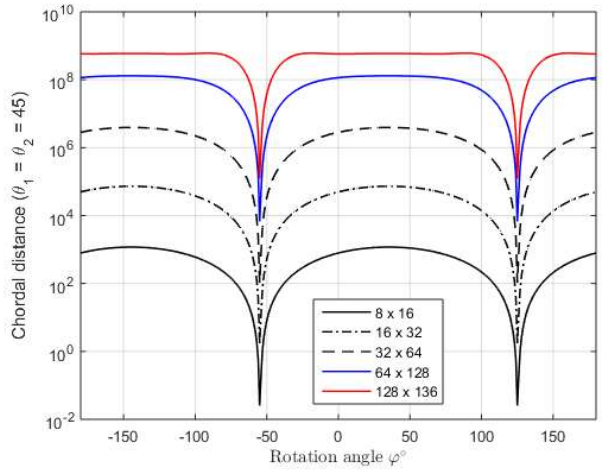

Figure 10: Chordal distance for different AAR configurations $(M_H \times M_V)$ vs. Rotation angle (ψ°) with equaled elevation angles ($\theta_1 = \theta_2 = 45°$) and unequaled azimuth angles ($\varphi_1 \neq \varphi_2$).

D. Impact of SE on AAR structure

Inter-user collinearity can have a positive impact on the SE since some users create less interference to each other. SE is the sum-rate (in bit/s/Hz) per user's channel and plays an important role in the network performance of the pure LoS massive MIMO networks.

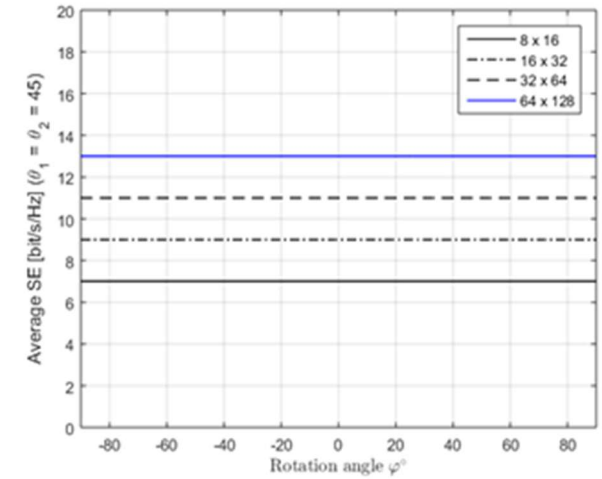

Figure 11: SE for different AAR configurations $(M_H \times M_V)$ vs. Rotation angle (ψ°) with equaled elevation angles ($\theta_1 = \theta_2 = 45°$) and unequaled azimuth angles ($\varphi_1 \neq \varphi_2$).

This metric is expressed in equation (11), we simulated numerically downlink sum SE by increasing the rotating angle in order evaluate the performance of the network. Figure 11 shows the simulation results of different AAR configurations $(M_H \times M_V)$ on the SE metric. Due to the MR precoding, the achievable SE is significantly higher for 64×128 antenna arrays compared to other antenna arrays because of significant amount of $|\rho|$ in the pure LoS. In case of 8×16,16×32, and 32×64 antenna arrays, the SIR is decreasing with increasing $|\rho|$, depicting the negative impact of ρ on the achievable SE with MR precoding using equation (11). This shows that the SE is decreased if two users are highly collinear.

E. Impact of CD on Array Antenna structure

The numerical results we have so far focused on CMD, CD, and the average SE. To study how the user correlation and choice of antenna array structure effect. The simulation results are obtained for the pure LoS scenario of the massive MIMO channel model. As shown in figure 12, the cumulative distribution function (CDF) of user correlation ($|\rho|$) for UPA, PPA, and AAR with different azimuth angles (φ) in two different scenarios. In the first scenario, $|\rho|$ is shown as function of ψ with different azimuth angles (φ_1= 22.5°, φ_2= 45°) and same elevation angles (θ_1, θ_2) at 45° for different AAR configurations $(M_H \times M_V)$.The 5th percentile |ρ| values of 8×16, 16×32, 32×64, 64×128 and 128×136 antenna arrays are 0.96, 0.86, 0.53, 0.03, and 0.00, respectively. This means that user correlation is inversely proportional to the number of antennas ($\rho = \frac{1}{M_H \times M_V}$) and can be achieved in practice. However, the larger the $M = M_H \times M_V$, the higher was the observed gap to the pure LoS case, giving rise to the conclusion that the marginal gain of additional M rapidly diminishes. Comparison of similar measurements were conducted by Akao *et al*. (2019) with different antenna architectures (horizontal, vertical, planar).

Table 4: 5th percentile vales of $|\rho|$ for AAR, PPA, and UPA antenna arrays

$M_H \times M_V$	AAR	PPA	UPA
8×16	0.9642	0.9961	1
16×32	0.8614	0.9961	1
32×64	0.5332	0.9961	1
64×128	0.0302	0.9961	1
128×136	0.0027	0.9961	1

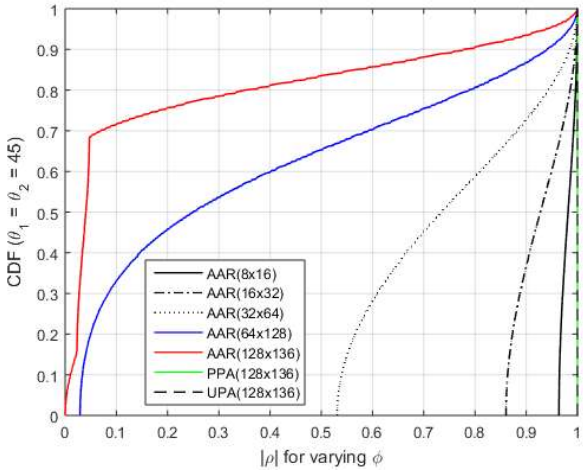

Figure 12: The CDF plots of user correlation ($|\rho|$) for UPA, PPA, and AAR when azimuth angles (φ) are varied from -90° to 90°.

In the second scenario, $|\rho|$ for both UPA and PPA with different azimuth angles (φ_1= 22.5°, φ_2= 45°), inter-element spacing ($d = 0.5\lambda$), column-wise offset ($d_r = 2\lambda$) and same elevation angles (θ_1, θ_2) at 45° respectively.The 5th percentile |ρ| values of both 128×136 UPA and 128×136 PPA antenna arrays are 0.9661 and 1, respectively as shown in figure 12 and table 4. We can see that spatial decorrelation of AAR is greater than UPA and PPA due to mechanical rotation of planar array according to channel spatial correlation.

F. Convergence Analysis

As briefly discussed in the algorithm section III, in order to evaluate the convergence of the proposed algorithm, the proposed algorithm is guaranteed to converge to an optimal rotating angle ψ_{OPT}. We used the recursive bisection algorithm (Mouatasim, 2017) for solving the min–max fairness problem (unconstrained optimization problem) with variables (12).

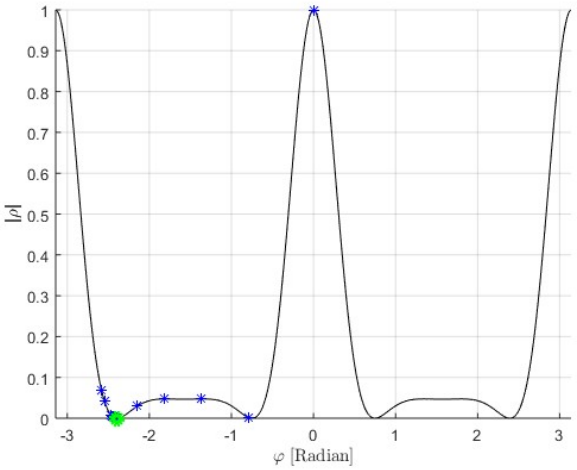

Figure 13: Spatial correlation $|\rho|$ for AAR configuration of M_H = 128 and M_V = 136 vs. rotating angle (ψ°) with same azimuth angles ($\varphi_1 = \varphi_2$) and different elevation angles ($\theta_1 \neq \theta_2$).

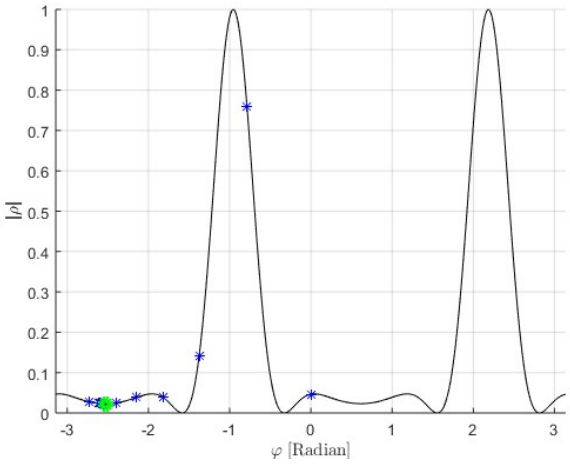

Figure 14: Spatial correlation $|\rho|$ for AAR configuration of M_H = 128 and M_V = 136 vs. rotating angle (ψ°) with different azimuth angles ($\varphi_1 \neq \varphi_2$) and same elevation angles ($\theta_1 = \theta_2$).

As presented in figures 13 and 14, the optimal line search process (i.e., blue asterisk) of algorithm 1 find by using recursive bisection method, we set $\Delta = 10^{-4}$ and $\psi = [-180°, 180°]$. We stop the iteration process, if we find the optimal rotating angles (i.e., green small circle) for elevation ($\psi_{OPT} = -2.392$ Radian or $-137.1°$) and azimuth ($\psi_{OPT} = -2.526$ Radian or $-144.7°$) scenarios. The conditions of the iteration process are satisfied when $\psi_{LOWER} = \psi_{UPPER} = \psi_{MIDPOINT}$ and percentage of error is zero. The iteration process results are listed in table 5 and table 6.

Table 5: Iteration process on Elevation Domain ($\psi_{OPT} = -2.392$ Radian or$-137.1°$)

n	ψ_{LOWER}	ψ_{UPPER}	$\psi_{MIDPOINT}$	SIGN	ERROR (%)
1	-3.142	1.568	-0.002	-0	-100
2	-3.142	0.391	-0.787	-1	-99.80
3	-3.142	-0.492	-1.375	-1	-42.81
4	-3.142	-1.155	-1.817	-1	-24.30
5	-3.142	-1.651	-2.148	-1	-15.42
6	-3.142	-2.024	-2.396	-1	-10.36
⋮	⋮	⋮	⋮	⋮	⋮
38	-2.392	-2.392	-2.392	-1	-0.000
39	-2.392	-2.392	-2.392	-1	-0.000

Table 6: Iteration process on Azimuth Domain ($\psi_{OPT} = -2.526$ Radian or$-144.7°$)

n	ψ_{LOWER}	ψ_{UPPER}	$\psi_{MIDPOINT}$	SIGN	ERROR (%)
1	-3.142	1.568	-0.002	-0	-100
2	-3.142	0.391	-0.787	1	-99.80
3	-3.142	-0.492	-1.375	0	-42.81
4	-3.142	-1.155	-1.817	-0	-24.30
5	-3.142	-1.651	-2.148	-0	-15.42
6	-3.142	-2.024	-2.396	-0	-10.36
⋮	⋮	⋮	⋮	⋮	⋮
38	-2.526	-2.526	-2.526	-0	-0.000
39	-2.526	-2.526	-2.526	-0	-0.000

The optimized rotation angles for AAR configuration of M_H = 128 and M_V = 136 with different values of constant elevation angles ($\theta_1 = \theta_2$) in azimuth domain are presented in table 7.

Table 7: ψ_{OPT} values for different constant elevation angles in azimuth domain

(φ_1, φ_2)	$\theta_1 = \theta_2$	ψ_{OPT}
22.5°,45°	90°(π/2)	−135° (-2.356)
22.5°,45°	60°(π/3)	−139° (-2.428)
22.5°,45°	45°(π/4)	−145° (-2.526)
22.5°,45°	36°(π/5)	−150° (-2.610)
22.5°,45°	30°(π/6)	−154° (-2.678)

One can verify or validate that the ψ_{OPT} can be successfully determined by the recursive bisection method.

V. CONCLUSION

This work has demonstrated the used of planar array antenna control method to simply decrease inter-user correlation by mechanical rotation of the antenna body in pure LoS environment. The research findings showed that inter-user correlation depends mainly on the angular separation and the antenna array geometry (antenna-element spacing, aperture). However, the amount of inter-user decorrelation and correlation behaviour with rotating angle are determined by the large number of antennas. A recursive bisection algorithm based on rotation angle optimization is proposed for LoS massive MIMO by finding the optimal antenna rotation angle. The numerical results depict significantly improved inter-user correlation performance which shifts the rotation of the antenna body in the azimuth domain and improves horizontal resolution. The 5th percentile $|\rho|$ values of antenna configuration for UPA and PPA antenna arrays are 0.9661 and 1 respectively. AAR reduces inter-user correlation by up to 99.7% for 128×136 arrays and 46.68% for 32×64 arrays. Moreover, the spatial decorrelation of AAR outperforms UPA and PPA due to mechanical rotation of planar array according to inter-user correlation. While this study confirms the effectiveness of AAR in pure LoS scenarios, future work may investigate its performance in mixed LoS/NLoS or scattering-rich environments. Additionally, implementing the mechanical rotation in practical hardware systems remains a design challenge.

AUTHOR CONTRIBUTIONS

G. C. Eze: Conceptualization, Methodology, Software, Validation, Writing – original draft, review & editing. **M. A. Ahaneku:** Supervision, Methodology, Software, Validation, Writing – review & editing. **V. C. Chijindu:** Supervision, Methodology, Software, Validation, Writing – review & editing.

REFERENCES

Akao, T.; K. Watanabe; S. Kojima; M. Katsuno; K. Maruta and C. Ahn. (2019). Reducing channel spatial correlation by rotating planar antenna array. Elsevier ICT Express, 5(1). Available online at https://doi.org/10.1016/j.icte.2019.03.004.

Arai, T.; A. Ohta; S. Kurosaki; K. Maruta; T. Iwakuni and M. Iizuka (2015). A new antenna arrangement design of massive MIMO in LOS environment for further capacity enhancement. Paper presented at 2015 9th European Conference on Antennas and Propagation (EuCAP), Lisbon.

Arai, T.; A. Ohta; Y. Shirato; S. Kurosaki; K. Maruta; T. Iwakuni and M. Iizuka. (2017). Antenna Array Arrangement for Massive MIMO to Reduce Channel Spatial Correlation in LOS Environment. IEICE Trans. Commun., April, E100–B (4).

Björnson, E.; J. Hoydis and L. Sanguinetti. (2017). Massive MIMO networks: Spectral, energy, and hardware efficiency. Found. Trends Signal Process. 11(3–4): 154–655.

Chien, T. V.; C. Mollén and E. Björnson. (2018). Large-scale-fading decoding in cellular massive MIMO systems with spatially correlated channels. arXiv:1807.08071. Available online at https://arxiv.org/abs/1807.08071

Farsaei, A.; A. Alvarado; Willems, F. M. J., and Gustavsson, U., (2019). An improved dropping algorithm for line-of-sight massive MIMO with Tomlinson-Harashima Precoding. IEEE Communications Letters, Nov., 23(11): 2099–2103.

Gao, X.; O. Edfors; F. Rusek and F. Tufvesson. (2011). Linear pre-coding performance in measured very-large MIMO channels. Paper presented at 2011 IEEE Vehicular Technology Conference (VTC Fall), Sep., 1–5.

Greving, G.; W. Biermann and R. Mundt (2012). Modeling and numerical analysis of rotating antennas and rotating scatterers applied to aeronautical system simulations. Paper presented at 2012 6th European Conference on Antennas and Propagation (EUCAP).

Hanada, T. and Maruta, K. (2020). Improving DOA Estimation Accuracy by Rotating Planar Array Antenna. Paper presented at IEEE Conference, October, 2020.

Henrik, A.; D. Astely; M. Buchmayer; P. V. Butovitsch; T. Chapman; S. Faxér; M. Frenne; C. Friberg; F. Ghasemzadeh; B. Göransson; M. Hagström; B. Hogan; Y. Jading; G. Jöngren; J. B Karlsson;E. Larsson; M. Ljungberg; J. Rao; J. Rosenberg; Y. Yang (2024). Introduction to Massive MIMO. The Massive MIMO handbook. The Third Edition, Ericsson AB. EN/LZT 4/28701-FGB1010987 Uen Rev C.

Honda, K. A (2021). Method of Implementing a 4 × 4 Correlation Matrix for Evaluating the Uplink Channel Properties of MIMO Over-the-Air Apparatus. Sensors 21:6184.

Farsaei, A.; A. Alvarado; F. M. J. Willems and U. Gustavsson (2019). An improved dropping algorithm for line-of-sight massive MIMO with max min power control. IEEE Communications Letters, Jun, 23(6):1109–1112.

Farsaei, A.; N. Amani; R. Maaskant; U. Gustavsson; A. Alvarado and F. M. J. Willems. (2020). Uniform Linear Arrays with Optimized Inter-Element Spacing for LOS Massive MIMO. IEEE Communications Letters.

Maruta, K.; T. Arai; A. Ohta; S. Kurosaki; T. Iwakuni and M. Iizuka. (2017). Experimental verification of massive antenna systems employing parallelogram planar arrays. IEEJ Transactions on Electrical and Electronic Engineering, Dec., 12 (S2):S82–S90. DOI:10.1002/tee.22568

Mouatasim, A. E. (2017). Implementation of reduced gradient with bisection algorithms for non-convex optimization problem via stochastic perturbation.Springer Science + Business Media.

Lin, Z.; T. Lv; W. Ni; J. A. Zhang and R. P. Liu. (2021). Nested hybrid cylindrical array design and DoA estimation for massive IoT networks.IEEE J. Sel. Areas Commun., Apr., 39(4): 919–933.

Lin, Z.; T. Lv; W. Ni; J. A. Zhang and R. P. Liu. (2020). Tensor-based multi-dimensional wideband channel estimation for mmWave hybrid cylindrical arrays. IEEE Trans. Commun., Dec., 68(12): 7608–7622.

Özdogan, Ö. ; E. Björnson and E. G. Larsson (2018). Uplink spectral efficiency of massive MIMO with spatially correlated Rician fading. Paper presented at Proc. SPAWC, Kalamata, Greece, Jun., 216–220.

Pratschner, S.; H. Groll; S. Caban; S. Schwarz and M. Rupp. (2020). Measured User Correlation in Outdoor-to-Indoor Massive MIMO Scenarios. IEEE Access. DOI:10.1109/ACCESS.2020.3026371

Pratschner, S.; T. Blazek; E. Zöchmann; F. Ademaj; S. Caban; S. Schwarz and M. Rupp. (2019). A Spatially Consistent MIMO Channel Model with Adjustable K Factor. IEEE Access, 7(1): 110174–110186.

Pratschner, S.; S. Caban; D. Schützenhöfer; M. Lerch; E. Zöchmann and M. Rupp. (2018). A fair comparison of virtual to full antenna array measurements. Paper presented at International Workshop on Signal Processing Advances in Wireless Communications (SPAWC), Kalamata, Greece, 1–5.

Riviello, D. G. and Garello, R. (2019a). Implementation of 5G beamforming techniques on cylindrical arrays. Paper presented at Proc. IEEE-APS Topical Conf. Antennas Propag. Wireless Commun. (APWC), Sep., 413–418.

Riviello, D. G. and Stasio, F. D. (2019b). 5G beamforming implementation and trade-off investigation of cylindrical array arrangements. Paper presented at Proc. 22nd Int. Symp. Wireless Pers. Multimedia Commun. (WPMC), Nov., 1–6.

Riviello, D. G.; R. Tuninato and R. Garello (2023). Assessment of MU-MIMO schemes with cylindrical arrays under 3GPP 3D channel model for B5G networks.in Proc. IEEE 20th Consum. Commun. Netw. Conf. (CCNC), Jan., 769–774.

Riviello, D. G.; R. Tuninato and R. Garello (2024). Multi-Layer Multi-User MIMO with Cylindrical Arrays under 3GPP 3D Channel Model for B5G/6G Networks. IEEE Access, 12.

Shafie, R.; M. J. Omidi; O. Abbasi and H. Yanikomeroglu (2024). MIMO-NOMA enabled sectorized cylindrical massive antenna array for HAPS with spatially correlated channels. IEEE Trans. Wireless Commun., early access, Jul. 23. doi: 10.1109/TWC.2024.3426521.

Shikhantsov, S.; A. Guevara and A. Thielens (2021). Spatial Correlation in Indoor Massive MIMO: Measurements and Ray-Tracing. IEEE Antennas and Wireless Propagation Letters. DOI 10.1109/LAWP.2021.3066607

Xu, J.; M. Li and R. Chen (2017). Space mapping optimisation of 2D array elements arrangement to reduce the radar cross-scattering. IET Microw. Antennas Propag., 11(11):1578–1582.

Yang, H., and Marzetta, T. L. (2017). Massive MIMO with max-min power control in line-of-sight propagation environment. IEEE Transactions on Communications, Nov., 65(11): 4685–4693.